Postnatal acquisition of endotoxin tolerance in intestinal epithelial cells

Michael Lotz,[1] Dominique Gütle,[1] Sabrina Walther,[1] Sandrine Ménard,[1,2] Christian Bogdan,[1] and Mathias W. Hornef[1,2]

[1]Department for Medical Microbiology and Hygiene, University Clinic of Freiburg, 79104 Freiburg, Germany
[2]Swedish Institute for Infectious Diseases Control, 17177 Stockholm, Sweden

The role of innate immune recognition by intestinal epithelial cells (IECs) in vivo is ill-defined. Here, we used highly enriched primary IECs to analyze Toll-like receptor (TLR) signaling and mechanisms that prevent inappropriate stimulation by the colonizing microflora. Although the lipopolysaccharide (LPS) receptor complex TLR4/MD-2 was present in fetal, neonatal, and adult IECs, LPS-induced nuclear factor κB (NF-κB) activation and chemokine (macrophage inflammatory protein 2 [MIP-2]) secretion was only detected in fetal IECs. Fetal intestinal macrophages, in contrast, were constitutively nonresponsive to LPS. Acquisition of LPS resistance was paralleled by a spontaneous activation of IECs shortly after birth as illustrated by phosphorylation of IκB-α and nuclear translocation of NF-κB p65 in situ as well as transcriptional activation of MIP-2. Importantly, the spontaneous IEC activation occurred in vaginally born mice but not in neonates delivered by Caesarean section or in TLR4-deficient mice, which together with local endotoxin measurements identified LPS as stimulatory agent. The postnatal loss of LPS responsiveness of IECs was associated with a posttranscriptional down-regulation of the interleukin 1 receptor–associated kinase 1, which was essential for epithelial TLR4 signaling in vitro. Thus, unlike intestinal macrophages, IECs acquire TLR tolerance immediately after birth by exposure to exogenous endotoxin to facilitate microbial colonization and the development of a stable intestinal host–microbe homeostasis.

CORRESPONDENCE
Mathias W. Hornef:
mathias.hornef@uniklinik-freiburg.de

Abbreviations used: HPRT, hypoxanthine phosphoribosyltransferase; IEC, intestinal epithelial cell; IRAK, IL-1 receptor–associated kinase 1; MIP-2, macrophage inflammatory protein 2; NEC, necrotizing enterocolitis; RQ, relative quantity; TLR, Toll-like receptor; ZO, zonula occludens protein.

Although an intimate relationship between members of the microbial flora and the intestinal epithelium has been documented, it is largely unknown how and to what extent the mucosal surface senses the presence of colonizing microbial organisms and allows for innate immune receptor-mediated responses (1). Recognition of microbial structures by mammalian cells occurs through various transmembrane receptor molecules that belong to the innate immune system. The Toll-like receptors (TLRs) recognize conserved microbial structures such as LPS, mediate cellular activation, and thereby provide the costimulatory signal required for an efficient immune response (2). Epithelial cells derived from colonized mucosal surfaces were initially thought to be devoid of these potent immunostimulatory receptors (3, 4). Later, TLR expression was also demonstrated on epithelial cells of the intestine and other tissues (5–8). However, functional studies were almost exclusively performed using established epithelial cell lines under conditions unable to reflect the complex environment in the gastrointestinal tract in vivo. Intact TLR signaling and microbial colonization was shown to support wound healing of colonic mucosal lesions (9, 10). The responsible $TLR4^+$ cell type was not identified, and recent work indicated intestinal macrophages as major players in colonic tissue repair (11). Thus, the characterization and functional relevance of TLR expression by the intestinal epithelium in vivo has remained unresolved.

In this study we investigated TLR4/MD-2 expression and LPS-mediated signaling in highly enriched primary small intestinal epithelial cells (IECs) of fetal, newborn, and adult mice. We used flow cytometry, intracellular chemokine staining, quantitative mRNA analysis, as well as stimulation assays to determine NF-κB activation, kinase activity, and chemokine synthesis in response to stimulation. We show that fetal, neonatal, and adult IECs express the TLR4/MD-2 receptor complex but dramatically differ in their

responsiveness to LPS. We describe for the first time the postnatal process of epithelial tolerance acquisition and identify the responsible molecular mechanism. This adaptive process is unique to epithelial cells because intestinal macrophages exhibited a constitutive, age-independent nonresponsive phenotype. The presented data support a new concept of the development of the enteric host–microbe homeostasis, which relies on postnatal acquisition of epithelial tolerance to microbial ligands to facilitate intestinal bacterial colonization. Moreover, the described findings might have a substantial impact on the understanding of the molecular processes that mediate mucosal host defense during microbial infection and tissue repair in the gastrointestinal tract.

RESULTS

Primary IECs age-independently express the LPS receptor TLR4/MD-2

To analyze TLR expression and ligand susceptibility, primary IECs were prepared from small intestinal tissue of C57BL/6 mice kept under specific pathogen-free conditions. Using a modified protocol for the isolation of intact intestinal epithelium, we were able to obtain viable, highly enriched preparations of differentiated epithelial cells (12, 13). Isolated epithelial cell aggregates showed the morphological features of intact intestinal villi with attached crypts. Phalloidin staining visualized apical actin fibers along the brush border microvilli (Fig. 1 A). Immunostaining illustrated the polarized phenotype with apically orientated lateral zonula occludens protein (ZO)-1 staining and broad lateral E-cadherin expression (Fig. 1 B). Viability and the absence of apoptosis in the majority of isolated IECs were confirmed by flow cytometric propidium iodine exclusion and negative annexin V staining (Fig. 1 C). IEC preparations were of high purity and contained only minute fractions of hematopoietic cells, such as T cells, B cells, or dendritic cells (Fig. 1 D), which was a prerequisite for the subsequent structural and functional analysis.

For the analysis of intestinal TLR expression, we first used laser microdissection to obtain IECs in situ from fetal, newborn, and adult enteric tissue. RT-PCR analysis revealed age-independent expression of the LPS receptor complex TLR4 and MD-2. Absence of contaminating TLR^+ myeloid cells in laser microdissection–derived epithelial cell preparations was shown by lack of CD45 expression (Fig. 2 A). Next, we prepared primary IECs from fetal and adult intestinal tissue as described above (Fig. 1), which were permeabilized and analyzed by flow cytometry confirming the expression of TLR4/MD-2. RAW 264.7 cells were used as a positive control (Fig. 2 B). To confirm the epithelial nature of the $TLR4^+$ cells, simultaneous staining for TLR4 and the epithelial cell marker E-cadherin was performed and revealed a great majority of double-positive cells (Fig. 2 C). Thus, epithelial cells in the intestinal tract express the LPS receptor TLR4/MD-2 in vivo.

Whereas macrophages carry the LPS recognition complex on the cell surface membrane, localization of TLR4 to the intracellular Golgi apparatus has been demonstrated in the IEC line m-IC_{cl2} (6). Immunostaining and flow cytometric analysis

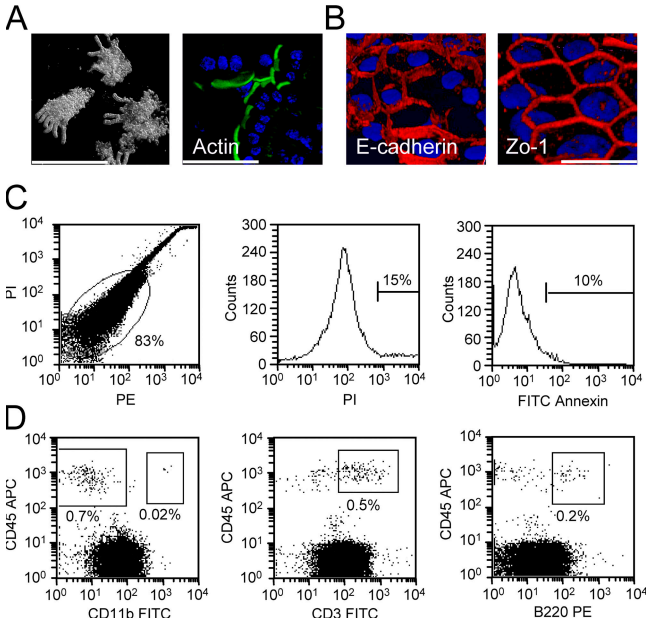

Figure 1. Characterization of primary IEC preparations. (A) Visualization of isolated primary epithelial cell aggregates comprising intestinal villi with the attached crypts by phase contrast microscopy. Bar, 1 μm. Phalloidin staining of freshly isolated primary cells illustrating actin accumulation along apical microvilli. Bar, 30 μm. (B) Verification of the polarized phenotype of primary IECs by immunostaining for E-cadherin (left) and ZO-1 (right). The depicted images show a three-dimensional reconstruction of the polarized, multicellular epithelial cell complex to illustrate the cellular structure. Bar, 10 μm. (C) Determination of cell viability and apoptosis of primary IECs by propidium iodine (PI) exclusion analysis and FITC–annexin V staining. (D) Staining for nonepithelial hematopoietic ($CD45^+$) cells of a representative preparation of primary IECs using anti-CD11b, anti-CD3, and anti-B220 antibodies.

of the same IEC preparations were performed under permeabilizing or nonpermeabilizing conditions to determine the cellular distribution of TLR4 in primary IECs. Peritoneal macrophages were used as control for cell surface localization. Whereas peritoneal macrophages exhibited strong cell surface staining for TLR4, the expression of TLR4 in viable primary IECs isolated from adult and fetal mice was clearly restricted to the intracellular space (Fig. 2 D). Because intracellular receptor localization would require ligand internalization, we next incubated primary IECs in the presence of *Salmonella typhimurium* LPS at a concentration of 100 ng/ml for 30 min. Indeed, the presence of intracellular LPS could be demonstrated using monoclonal antibodies directed against the *S. typhimurium* LPS O4 and O5 antigen (Fig. 2 E). Thus, expression of TLR4 in viable primary IECs is restricted to an intracellular compartment, and ligand internalization might facilitate stimulation as recently shown for intestinal epithelial m-IC_{cl2} cells (14).

IECs exhibit differential susceptibility to LPS depending on the developmental stage

To analyze whether IECs sense and respond to the presence of microbial ligands, we first tested the production of the

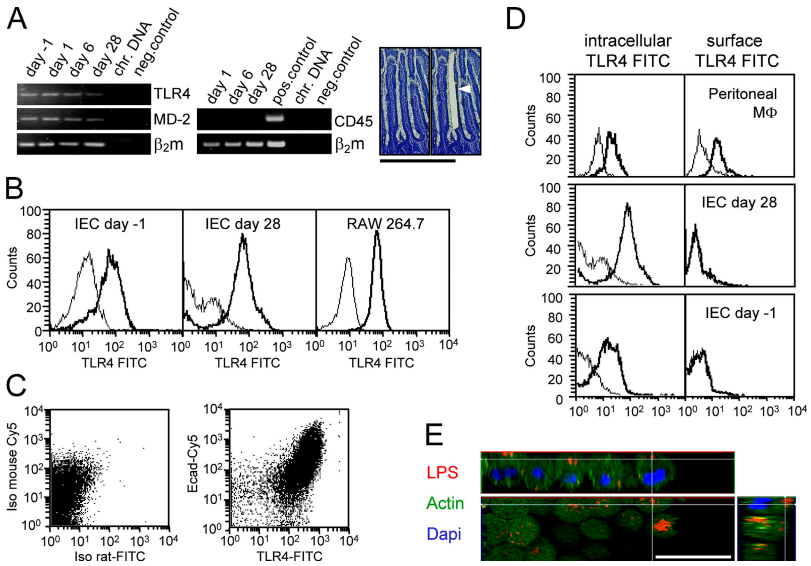

Figure 2. Intracellular LPS receptor expression by primary IECs. (A) RT-PCR analysis for TLR4 and MD-2 expression in intestinal epithelium from fetal, 1-, and 6-d-old newborn as well as adult intestinal tissue obtained by laser microdissection. Detection of CD45 expression was used to demonstrate the absence of myeloid cells in the dissected tissue. Macrophage-like RAW 264.7 cells were used as positive control for CD45 expression. β_2-microglobulin (β_2m) expression was used as a housekeeping control. The hematoxylin-stained tissue section illustrates the microdissection procedure. Bar, 500 μm. (B) FACS analysis of isolated primary IECs from fetal (day −1) and adult (day 28) murine intestine for the expression of the LPS receptor complex TLR4/MD-2. RAW 264.7 cells were used as positive control. Dotted line, isotype control. (C) FACS analysis using double immunostaining of primary IECs for isotype antibodies (left) or TLR4/MD-2 and E-cadherin (right) to confirm epithelial TLR4 expression. Primary IECs were isolated from 6-d-old mice. (D) Staining of murine peritoneal macrophages as well as primary IECs isolated from adult (day 28) and fetal (day −1) intestinal tissue for TLR4/MD-2 with or without permeabilization of the cellular membrane to illustrate surface TLR expression. Dotted line, isotype control. (E) LPS internalization of primary IECs. Cells were incubated in the presence of 100 ng/ml *S. typhimurium* LPS and immunostained using two monoclonal antibodies directed against the LPS O-antigen. Counterstaining with FITC-phalloidin and DAPI. Bar, 20 μm.

proinflammatory chemokines KC and macrophage inflammatory protein 2 (MIP-2), functional murine homologues of the human IL-8. No chemokines were measurable in supernatants of resting IECs isolated from adult mice. Also, stimulation with LPS or the cytokines TNF or IL-1β did not result in detectable chemokine secretion (Fig. 3 A). This nonresponsive phenotype could not be overcome by the addition of high concentrations of LPS (1–5 μg/ml; not depicted). In striking contrast, primary IECs from fetal intestinal tissue readily responded to LPS, IL-1β, or TNF with a significant increase of chemokine secretion (Fig. 3 B). Activation was seen with LPS concentrations as low as 10 ng/ml, illustrating the susceptibility of fetal primary cells to LPS. Although exposure to other TLR ligands also resulted in cellular activation, LPS represented the most potent stimulus (not depicted). Primary IECs from newborn mice (1–6-d-old) exhibited spontaneous chemokine secretion, which, however, could not be enhanced by the addition of LPS or immunostimulatory cytokines (Fig. 3, C and D). Additionally, LPS and cytokine-mediated phosphorylation of NF-κB signaling molecules were analyzed in fetal and adult primary IECs. Whereas rapid phosphorylation of IκB-α and the NF-κB subunit p65 was noted upon stimulation of fetal IECs with 100 ng/ml LPS or 50 ng/ml TNF, IECs isolated from adult tissue were completely unresponsive (Fig. 3 E).

To exclude the possibility that the chemokines in the culture supernatant or the detected kinase activity might originate from minor hematopoietic contaminants within the epithelial cell preparation, intracellular chemokine staining was established. Control experiments using naive or LPS-stimulated primary peritoneal macrophages confirmed the validity of the method for the detection of MIP-2 production (Fig. 4 A). Primary IECs prepared from late gestational fetuses (day −1), 6-, or 28-d-old mice were incubated in the presence or absence of 100 ng/ml LPS, stained for intracellular MIP-2, and examined by FACS analysis (Fig. 4 B). Similar to the chemokine secretion assays, MIP-2 production in nonstimulated cells was only observed in IECs from 6-d-old newborn mice, but not in cells from fetal or adult animals (Fig. 4 B, left column). In contrast, LPS exposure induced MIP-2 staining in primary IECs from fetal tissue, but not in IECs isolated from adult mice. No further increase of the spontaneous chemokine production by LPS stimulation was detected in IECs isolated from 6-d-old newborn mice (Fig. 4 B, right column). Finally, double staining of 6-d-old newborn IECs for E-cadherin and intracellular MIP-2 unequivocally demonstrated that IECs were the source of chemokine production (Fig. 4 C). This was also confirmed by immunofluorescence visualizing MIP-2^+ cellular compartments in E-$cadherin^+$ primary IECs (Fig. 4 D). In conclusion, fetal but not adult IECs exhibit susceptibility to

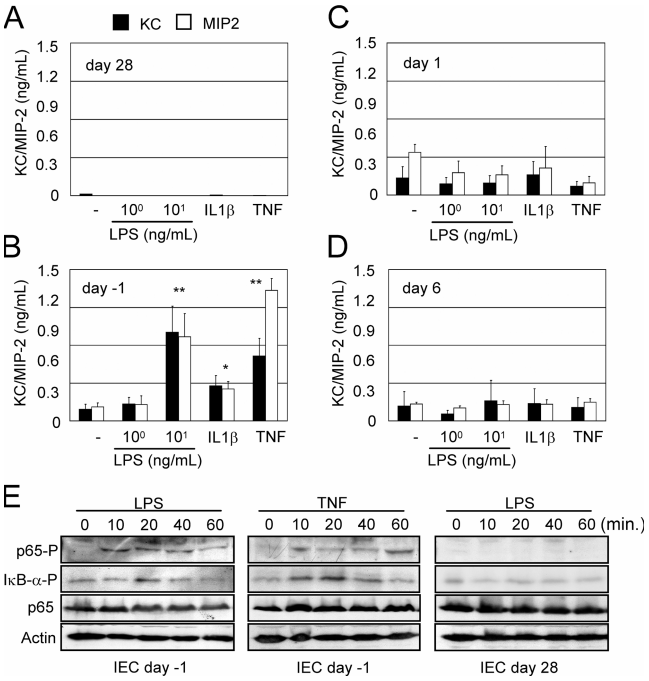

Figure 3. Stimulation of isolated primary IECs. MIP-2 and KC concentrations in the cell culture supernatant of primary IECs isolated from adult mice (day 28; A), late gestational fetuses (day −1; B), newborn mice (day 1; C), or 6-d-old mice (D). Cells were stimulated with 1 or 10 ng/ml LPS, 100 ng/ml IL-1β, or 50 ng/ml TNF for 12 h. Values are presented as means ± SD. *, $P < 0.05$; **, $P < 0.01$. (E) Immunoblot analysis of p65 and IκB-α phosphorylation in primary IECs isolated from fetal (day −1) or adult (day 28) mice 10, 20, 40, and 60 min after stimulation with 100 ng/ml LPS or 50 ng/ml TNF. Equal sample loading is illustrated by actin and total p65 staining.

LPS stimulation and IECs isolated from newborn mice show spontaneous activation.

Intestinal macrophages are constitutively nonresponsive to LPS

Resident intestinal macrophages from adult patients do not release proinflammatory mediators in response to microbial stimulation (15). To examine whether intestinal macrophages similar to IECs acquire nonresponsiveness only after birth, we analyzed the secretion of proinflammatory cytokines as well as the expression of costimulatory molecules on isolated fetal, neonatal, and adult $CD45^+$ and $BM8^+$ primary intestinal macrophages (Fig. 5 A). Flow cytometric analysis of the costimulatory activation markers CD40 and B7.1 (CD80) on intestinal macrophages from fetal, 1-, 3-, and 28-d-old mice revealed no postnatal up-regulation (Fig. 5 B). Also, in vitro stimulation of fetal intestinal macrophages with LPS did not lead to significant up-regulation of CD40 or B7.1, whereas strong up-regulation of both markers was noted after stimulation of the macrophage-like cell line RAW 264.7 (Fig. 5 C). Finally, LPS stimulation of blood monocytes, but not of fetal intestinal macrophages, revealed secretion of significant levels of the proinflammatory cytokines MIP-2 and TNF (Fig. 5, D and E). Thus, in contrast to IECs that acquire LPS resistance only during the course of a postnatal activation process, intestinal macrophages exhibit a constitutive nonresponsiveness to LPS that reflects the influence of tissue origin.

Intestinal epithelial activation occurs in vivo immediately after birth

Shortly after birth, the sterile body surfaces of the newborn become exposed to organic substances from the microbially colonized environment. Also, we have shown that IECs from newborn mice spontaneously release inflammatory chemokines (see Fig. 3 C). To further delineate the mechanistic basis and kinetics of this transient activation, RNA was isolated from mice before and 1, 3, 6, and 15 d after birth and quantitatively analyzed for the presence of MIP-2 mRNA. A transient three- to fourfold increase of MIP-2 expression was seen in the total RNA isolated from the small intestine at the first day of life (Fig. 6 A). This mRNA induction was significantly more pronounced in isolated IECs than in total small intestine, identifying IECs as a primary source of mRNA synthesis (Fig. 6 B). To identify the exact time point of maximal epithelial stimulation, RNA was harvested from the small intestine of littermates at 0, 1, 2, 4, and 6 h after birth. Strikingly, quantitative MIP-2 mRNA analysis revealed a maximal increase at 2 h after birth followed by rapid normalization within 6 h (Fig. 6 C). To confirm the time course and verify transcriptional activation of the epithelium, the cellular localization of the NF-κB subunit p65 as well as phosphorylation of IκB-α were analyzed in situ by immunostaining of intestinal tissue obtained shortly after natural delivery. Indeed, whereas p65 localized to the cytoplasma directly after birth, nuclear translocation of p65 was detected in situ in IECs within 60 min after delivery (Fig. 6 D). Also, phosphorylation of IκB-α was detected in IECs 45 and 60 min after birth (Fig. 6 E). Although cellular activation as reflected by transcriptional up-regulation and protein synthesis of the chemokine MIP-2 revealed a potent immunostimulation, no increase of $CD45^+$ inflammatory cells in intestinal tissue was noted after birth (Fig. 6 F). Thus, a strong, self-limited transcriptional activation of IECs was observed in neonatal mice shortly after birth in the absence of an inflammatory reaction.

Postnatal epithelial activation depends on exogenous microbial ligand exposure

To analyze the potential impact of exogenous microbial ligands for the observed postnatal epithelial activation, we compared vaginally born neonatal mice with mice that were delivered by Caesarean section and not exposed to maternal body fluids or environmental stimuli. Strikingly, postnatal epithelial MIP-2 induction was only detected in naturally born mice but completely absent in 2-h-old neonatal mice that were delivered by Caesarean section and kept separately from adult animals (Fig. 7 A). To quantitatively analyze the concentrations of microbial ligands in intestinal

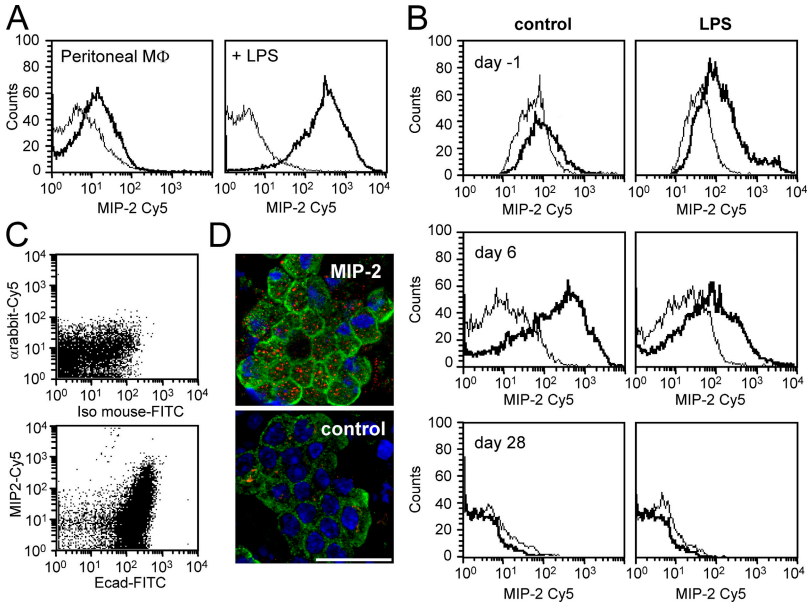

Figure 4. Transient postnatal activation and LPS susceptibility of primary IECs. (A) Characterization of intracellular MIP-2 staining using nonactivated or LPS (100 ng/ml) -stimulated peritoneal macrophages. (B) Intracellular MIP-2 staining of primary IECs isolated from late gestational fetal, 6-, and 28-d-old mice. MIP-2 was cytometrically analyzed after 6 h of incubation in the presence of brefeldin A under nonstimulating conditions or after the addition of 100 ng/ml LPS. Dotted line, isotype control. (C) Double immunostaining and FACS analysis of primary IECs from 6-d-old mice with MIP-2 and E-cadherin to identify spontaneous MIP-2 production in IECs. (D) MIP-2 (red) in IECs from 6-d-old mice was detected by intracellular staining with a rabbit anti–MIP-2 antiserum (MIP-2) or an irrelevant affinity-purified rabbit control serum after incubation for 6 h in the presence of 0.5 μg/ml brefeldin A. Isolated IECs were identified as epithelial cells by E-cadherin staining (green). Counterstaining with DAPI. Bar, 20 μm.

tissue, a sensitive colorimetric limulus-endotoxin test was performed. Considerable endotoxin concentrations (nanograms per gram tissue) were measured in homogenates of neonatal intestine shortly after birth (Fig. 7 B). As a possible source for microbial ligands, the gastrointestinal tract of adult animals was also examined and exhibited dramatic amounts of biologically active endotoxin (Fig. 7 C). To verify the role of exogenous microbial ligands, we next exposed Caesarean-born neonates orally to low amounts of endotoxin. Indeed, oral exposure to LPS evoked a rapid increase of MIP-2 mRNA in the intestinal tissue of Caesarean-born neonates, similar to the situation in vaginally born mice (Fig. 7 D). Thus, LPS alone is able to evoke IEC stimulation. To evaluate the contribution of LPS for epithelial activation in vivo, we further analyzed mice deficient in TLR4. Surprisingly, lack of TLR4 resulted in an almost complete lack of epithelial activation (Fig. 7 E). Thus, the observed postnatal epithelial stimulation depends on vaginal delivery, oral exposure to endotoxin, and the presence of TLR4.

Postnatal activation is controlled by posttranscriptional down-regulation of IL-1 receptor–associated kinase 1 (IRAK-1)

Both the rapid normalization of transcriptional cell activation as well as the lack of inflammatory tissue infiltration prompted us to analyze the involvement of known negative regulators of TLR signaling. We first screened for a postnatal up-regulation of Sigirr and ST-2 expression as well as for the appearance of the differentially spliced short form of MyD88 (sMyD88) (16–18). All three membrane proteins exert their inhibitory function by interaction with proximal signaling molecules of the IL-1R/TLR signaling pathway. Constitutive expression of Sigirr and ST-2 mRNA was detected in epithelial cells obtained by laser microdissection (not depicted). Also, no transcript of sMyD88 could be amplified from neonate intestinal tissue (not depicted). The cytoplasmic protein Tollip has been shown to interact with MyD88 and is the only inhibitory molecule known to exert a negative regulatory effect on TLR signaling in epithelial cells (19). However, Tollip mRNA levels in intestinal tissue remained unchanged during the postnatal period. Also, the amount of Tollip protein detected in fetal and neonatal intestinal tissue or the corresponding isolated IECs remained unchanged after birth (not depicted). Finally, whereas Tollip was up-regulated by LPS stimulation of RAW 264.7 cells, no increase was found in mouse intestinal epithelial m-IC_{cl2} cells (not depicted). Thus, none of the transcriptionally regulated inhibitory molecules could be identified to play a significant role in postnatal epithelial tolerance.

Transient posttranscriptional down-regulation of the TLR signaling molecule IRAK-1 has been associated with acquired hyporesponsiveness in macrophages (20–22). However, IRAK-1 levels in total intestinal tissue of fetal and postnatal tissue remained unchanged (not depicted). Surprisingly, evaluation of isolated primary IECs demonstrated rapid

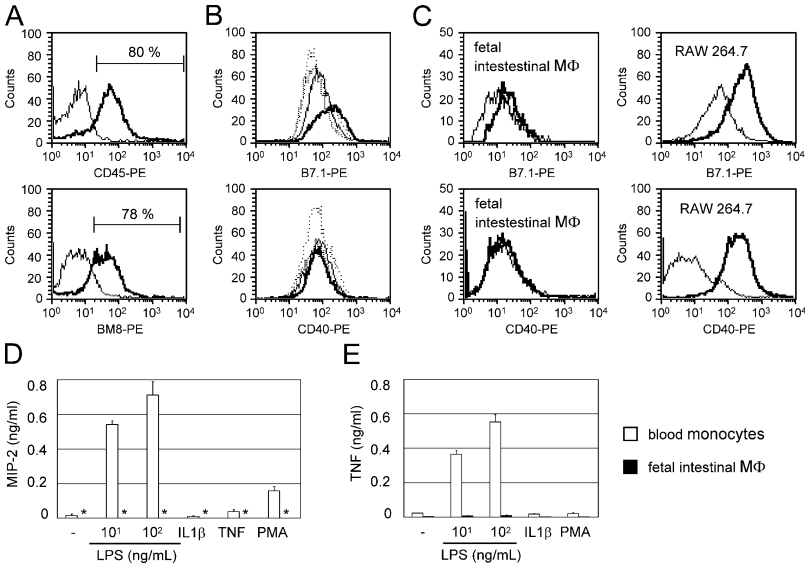

Figure 5. Constitutive LPS resistance of intestinal macrophages. (A) Characterization of the isolated intestinal macrophage preparation by CD45 (top) and BM8 (bottom) expression. (B) Analysis of surface B7.1 (top) and CD40 (bottom) expression on intestinal macrophages from fetal (bold), 1- (normal), 3- (thin), and 28-d-old (dotted line) mice. (C) B7.1 (top) and CD40 (bottom) expression on fetal intestinal macrophages (left) and RAW 264.7 cells (right) after overnight incubation in the absence or presence of 100 ng/ml LPS. MIP-2 (D) and TNF (E) secretion by blood monocytes and intestinal macrophages from fetal mice after overnight stimulation with LPS, 100 ng/ml IL-1β, 50 ng/ml TNF, and phorbol ester (5 μM PMA). *, not detectable.

down-regulation of IRAK-1 protein after birth, whereas the IRAK-1 mRNA expression remained stable throughout the examined time course (Fig. 8, A and B). IRAK-1 down-regulation was confirmed by immunostaining of IRAK-1 in fetal and postnatal intestinal tissue (Fig. 8 C). Similar to primary IECs, a poststimulatory depletion of IRAK-1 was also found in macrophage-like RAW 264.7 cells (Fig. 8 D) and even more pronounced in intestinal epithelial m-IC_{cl2} cells (Fig. 8, E and F). In accordance with recent results obtained studying myeloid cells, preincubation of IECs with the kinase inhibitor K-252b inhibited IRAK-1 degradation (Fig. 8 G; reference 23). In addition, ubiquitination of IRAK-1 was detected in LPS-exposed ubiquitin-overexpressing m-IC_{cl2} cells by immunoprecipitation (Fig. 8 H). Together, posttranscriptional down-regulation of IRAK-1 in response to microbial stimulation was observed in IECs and might be responsible for the rapid termination of postnatal epithelial cell activation and thereby prevent prolonged chemokine production and the attraction of professional immune cells.

IRAK-1 is essential for epithelial TLR4 signaling, and down-regulation contributes to endotoxin tolerance

A role of IRAK-1 for impaired IL-1R/TLR and TNF receptor signaling has previously been shown in IRAK-1–deficient mice and isolated macrophages (24–27). However, the general hyporesponsive phenotype of IRAK-1–deficient mice precluded their use for the analysis of the role of IRAK-1 for the acquisition of epithelial tolerance in vivo. Therefore, we resorted to an in vitro model of tolerance induction using differentiated intestinal m-IC_{cl2} epithelial cells (6). As seen before, LPS stimulation of nontransfected or mock-transfected m-IC_{cl2} cells conferred nonresponsiveness to a second LPS stimulus (Fig. 9 A). When a dominant-negative construct of IRAK-1 was transfected into LPS-susceptible m-IC_{cl2} cells before LPS stimulation, a substantial reduction of LPS-induced MIP-2 secretion was noted that was in accordance with the 30–40% transfection efficiency obtained in m-IC_{cl2} cells (Fig. 9 A). Cotransfection of an NF-κB luciferase reporter construct together with the dominant-negative form of IRAK-1 resulted in an even more pronounced reduction of cellular activation (Fig. 9 B). In addition, the effect of overexpression of IRAK-1 on the susceptibility of tolerant m-IC_{cl2} cells was evaluated. Whereas nontransfected or mock-transfected cells exhibited significantly reduced LPS sensitivity after LPS tolerization, overexpression of IRAK-1 in tolerant cells almost completely rescued LPS susceptibility (Fig. 9 C). The restored responsiveness to LPS was accompanied by detectable amounts of IRAK-1 in cell lysate (Fig. 9 D). Finally, the effect of IRAK-1 overexpression on NF-κB p65 translocation in tolerant m-IC_{cl2} cells was analyzed on the cellular level. Whereas tolerant cells exhibited a strongly reduced LPS susceptibility as compared with naive cells, intact nuclear translocation of p65 was observed in tolerant cells overexpressing IRAK-1 (Fig. 9 E). Thus, IRAK-1 plays an essential role during LPS activation of IECs, and lack of IRAK-1 in tolerant cells significantly contributes to the LPS-resistant phenotype.

DISCUSSION

TLR-mediated recognition of conserved microbial structures and ligand-induced cellular activation was first discovered

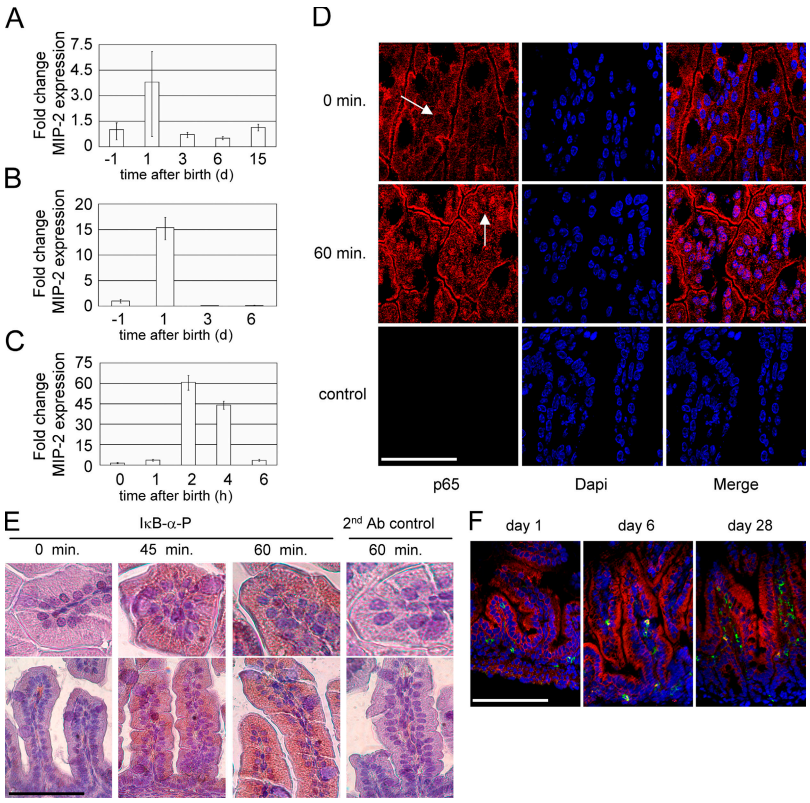

Figure 6. Time course of postnatal IEC activation. (A) Quantitative MIP-2 mRNA analysis in total small intestinal tissue from fetal, 1-, 3-, 6-, and 15-d-old mice. HPRT expression was used for normalization. Values are presented as RQ ± RQ maximum and minimum, respectively, and indicate MIP-2 mRNA expression relative to the fetal tissue sample. (B) Quantitative MIP-2 mRNA analysis in isolated primary IECs from fetal, 1-, 3-, and 6-d-old mice. (C) Quantitative MIP-2 mRNA analysis in total small intestinal tissue 0, 1, 2, 4, and 6 h after birth. (D) Immunostaining of neonatal small intestinal tissue obtained 0 and 60 min after delivery. The arrows indicate the cytoplasmic (0 min) or nuclear (60 min) cellular distribution of the NF-κB subunit p65. A secondary antibody control illustrates the specificity of the immunostaining. Counterstaining with DAPI. Bar, 50 μm. (E) Immunostaining for phosphorylated IκB-α in neonatal small intestinal tissue obtained 0, 45, and 60 min after delivery. Counterstaining with hematoxylin. Bar, 100 μm. (F) Immunostaining of small intestinal tissue from 1-, 6-, and 28-d-old mice for the presence of $CD45^+$ (green) immune cells. Counterstaining with TRITC-phalloidin. Bar, 250 μm.

on professional immune cells such as macrophages and dendritic cells that reside in largely sterile tissue environments (27). The situation on epithelial surfaces, however, is markedly different. The intestinal tract is exposed to a variety of environmental microbial ligands and is colonized by a dense, complex, and highly dynamic microbial flora that contributes to the intestinal physiology by substrate degradation and synthesis of essential nutrients (28). The composition of the microbial flora is complex and provides most of the identified innate immune receptor ligands such as LPS at high concentrations. Thus, innate immune recognition within the gastrointestinal tract must be tightly regulated to avoid inappropriate stimulation.

The vast majority of previous studies on TLR-mediated recognition by epithelial cells have been performed using established cell lines under cell culture conditions and resulted in a heterogenous picture of TLR expression and ligand susceptibility (29). In contrast, the use of mouse chimera with myeloid cell–restricted TLR expression indicated an important contribution of lung and bladder epithelial cells for the TLR4-mediated host microbe interaction (30, 31). In the present study, we performed a detailed in vivo characterization of primary IECs within their complex natural environment by using laser microdissection, immunohistology, as well as ex vivo assays with isolated epithelial cells. LPS stimulation of fetal IECs in vitro readily resulted in intracellular cell signaling, transcriptional activation, as well as chemokine synthesis and secretion. However, LPS susceptibility of IECs was lost after birth, indicating perinatal induction of negative regulatory control mechanisms of epithelial TLR signaling. This unique adaptive phenotype of epithelial cells with a postnatal acquisition of TLR resistance is further illustrated by the strikingly different situation found in intestinal macrophages. Intestinal macrophages exhibited a constitutive, age-independent nonresponsive phenotype that appears to be causally related to their tissue localization. Therefore, the observed postnatal activation represents a previously unrecognized epithelium-specific adaptive process that might play an important role to facilitate postnatal microbial colonization and establishment of a stable homeostasis on intestinal surfaces.

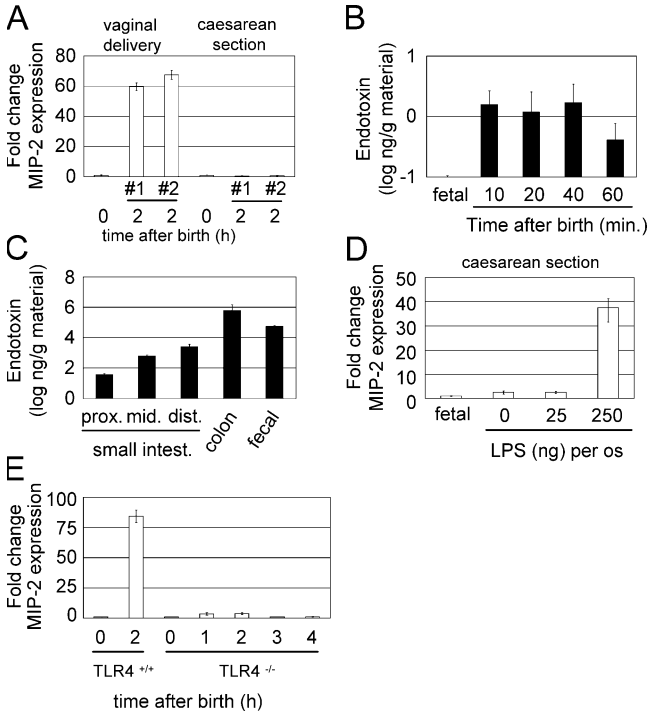

Figure 7. Characterization of the stimulus of postnatal epithelial activation. (A) Quantitative MIP-2 mRNA analysis in total small intestinal tissue of newborn mice 0 and 2 h after vaginal delivery or Caesarean section. #1 and #2 identify individual mice examined. (B) LPS concentration in total small intestinal homogenate of normally delivered newborn mice at the indicated time after birth. (C) LPS concentration in intestinal content and fecal samples of adult mice ($n = 4$). (D) Quantitative MIP-2 mRNA analysis in total small intestinal tissue of fetal or neonatal mice born by Caesarean section 3 h after oral exposure to LPS at the indicated concentrations. (E) Quantitative MIP-2 mRNA analysis in total small intestinal tissue of wild-type as well as TLR4-deficient newborn mice after vaginal delivery.

Consistent with the LPS-susceptible phenotype of fetal IECs, exposure to the nonsterile environment after birth led to activation of the intestinal epithelium. However, the rapid, strong, and transient response observed in vivo within 2 h after birth was unexpected. In fact, nuclear translocation of the NF-κB subunit p65 was observed already at 60 min after birth, indicating stimulation in close context with the delivery process. Analysis of neonates born by Caesarean section suggested an exogenous stimulus. LPS measurements in newborn intestinal tissue, the stimulatory effect of oral LPS exposure in Caesarean-born neonates, as well as the absence of epithelial activation in TLR4-deficient mice finally identified LPS as the major microbial stimulus for postnatal epithelial activation. The high concentrations of biologically active endotoxin in intestinal and fecal samples of adult animals illustrated the minute volumes of ingested contaminated material required to evoke stimulation. However, although clearly the predominant stimulus, endotoxin might act in synergism with other microbial compounds in vivo. It is tempting to speculate that the observed postnatal epithelial activation might also occur on other epithelial body surfaces and could be involved in the up-regulation of host defense molecules to prepare for subsequent microbial exposure.

The activation of IECs after birth showed a self-limited time course with MIP-2 mRNA levels returning to baseline within only 4–6 h after delivery and no detectable proinflammatory tissue infiltration. Thus, the observed epithelial stimulation induced a potent negative regulatory mechanism that caused rapid termination of cellular activation and induced unresponsiveness to subsequent stimulation. Posttranscriptional down-regulation of IRAK-1 was detected selectively in primary IECs shortly after birth, and in vitro studies using differentiated intestinal epithelial m-IC_{cl2} cells suggested that posttranscriptional depletion of IRAK-1 might significantly contribute to the observed LPS nonresponsive phenotype of primary postnatal IECs. IRAK-1 together with IRAK-4 binds to the TLR/adaptor molecule complex and transmits the signal to the TNF receptor–associated factor 6 to facilitate NF-κB activation (32). The important role of IRAK-1 for IL-1 receptor/TLR-mediated signaling has been demonstrated using IRAK-1–deficient mice (24–26, 33). Interestingly, earlier work also revealed an important role of IRAK-1 for TNF receptor signaling (27). Although IRAK-1 down-regulation upon LPS stimulation has previously been noted in macrophages, our study is the first report to identify IRAK-1 depletion in epithelial cells as a mechanism of TLR hyporesponsiveness in vivo (20–22).

A recent study demonstrated that large amounts of LPS given orally induced intestinal pathology with significant mortality in fetal and newborn rats, but not in older animals (34). LPS susceptibility of fetal IECs has also been observed in humans (35, 36). Thus, postnatal epithelial activation might also occur in humans, and dysfunction of negative regulation and tolerance acquisition, e.g., in undifferentiated enterocytes, or increased stimulation by enhanced stimulus concentration might lead to the development of enteric inflammation. A corresponding clinical picture is seen in patients with necrotizing enterocolitis (NEC), a devastating inflammatory disease of the intestine frequently seen in premature newborns. NEC is characterized by enteric cytokine production, polymorphonuclear cell (PMN) activation, tissue infiltration, ischemic hemorrhage, and high mortality (37). Microbial colonization, enteral feeding, hyperresponsiveness of immature enterocytes, and uncontrolled cytokine production have been proposed to contribute to the pathogenesis of this disease, although its exact etiology has remained unclear (38). Our data suggest that dysregulation of the observed postnatal proinflammatory epithelial activation might participate in the pathogenesis of NEC.

In conclusion, this study provides conclusive evidence that primary IECs express TLR4 and are able to respond to LPS in vivo. It is the first to describe spontaneous postnatal epithelial cell activation induced by exogenous endotoxin and identifies posttranscriptional down-regulation of IRAK-1 as a negative regulatory mechanism of TLR4 signaling in IECs in vivo. This adaptive process might be crucial to

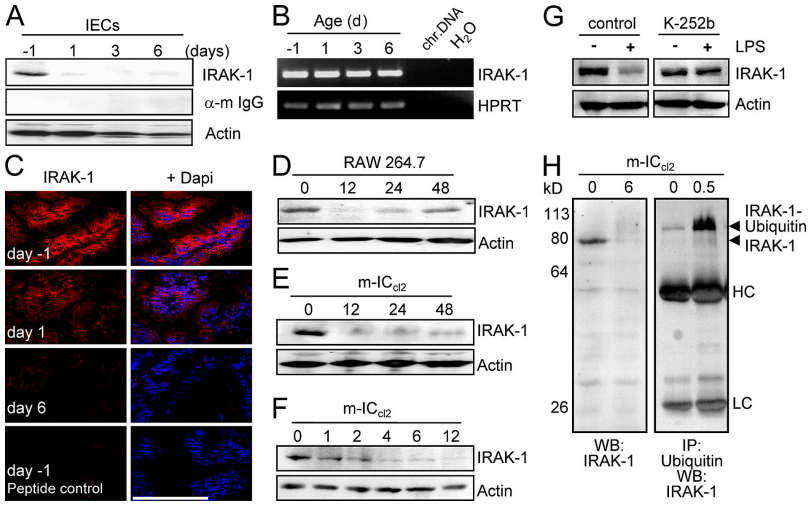

Figure 8. Postnatal depletion of IRAK-1 in IECs. (A) Immunoblot for IRAK-1 in primary IECs isolated from fetal (day −1), 1-, 3-, and 6-d-old mice. A secondary antibody control was included to demonstrate the specificity of the IRAK-1 staining. Actin was included as loading control. (B) Analysis of IRAK-1 expression in LMD-isolated primary IECs. HPRT was included as housekeeping control. (C) Immunostaining for IRAK-1 in small intestinal tissue of fetal (day −1), 1-, and 6-d-old mice. A peptide control illustrates the specificity of the immunstaining. Counterstaining with DAPI. Bar, 100 μm. (D–F) Immunoblot for IRAK-1 in macrophage-like RAW 264.7 cells and mouse intestinal epithelial m-IC_{cl2} cells at the indicated time points (hours) after exposure to 100 ng/ml LPS. (G) Immunoblot for IRAK-1 in mouse intestinal epithelial m-IC_{cl2} cells 2 h after exposure to 100 ng/ml LPS in the absence or presence of 25 μM of the kinase inhibitor K-252b. Actin was included as loading control. (H) Immunoblot for IRAK-1 in mouse intestinal epithelial m-IC_{cl2} cells left untreated or stimulated with 100 ng/ml LPS for 6 h (left). m-IC_{cl2} cells transfected with an ubiquitin expression plasmid and stimulated with 100 ng/ml LPS for 0 or 0.5 h were immunoprecipitated using a polyclonal anti-ubiquitin antibody and immunoblotted to visualize IRAK-1 (right). Note the size difference between native and ubiquitinated IRAK-1. HC, heavy chain; LC, light chain.

facilitate postnatal microbial colonization and subsequent development of the astonishingly stable, lifelong symbiosis. The finding that epithelial unresponsiveness of postnatal IECs is not intrinsically determined, but acquired, illustrates the requirement for effective negative regulatory mechanisms of innate immune recognition by IECs to prevent inflammatory disease. In addition, the newly discovered epithelial activation shortly after birth might pose a significant risk for individuals

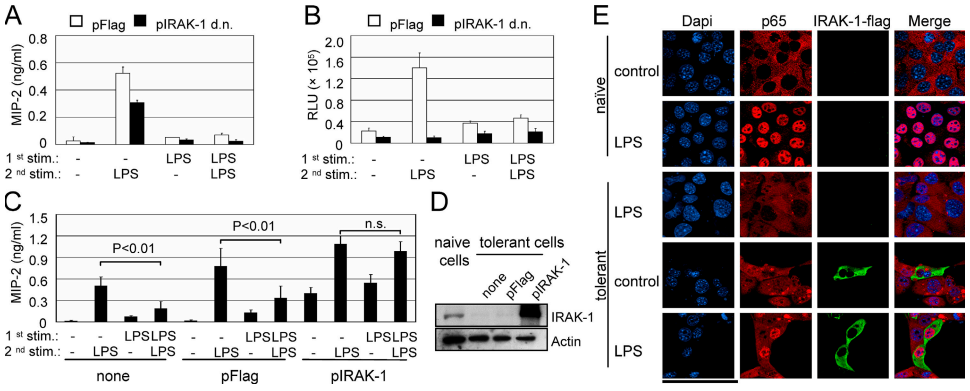

Figure 9. Role of IRAK-1 in epithelial TLR4 signaling and endotoxin tolerance. (A) MIP-2 secretion of intestinal epithelial m-IC_{cl2} cells transfected with a control plasmid or a dominant-negative construct of IRAK-1. Cells were initially incubated in the presence or absence of 1 μg/ml LPS for 6 h, recovered for 36 h in LPS-free medium, and restimulated with 100 ng/ml LPS for 6 h. (B) Cotransfection of a dominant-negative version of IRAK-1 with an NF-κB luciferase reporter construct. Luciferase production in response to LPS stimulation of naive and LPS-tolerant cells carrying a control plasmid or a dominant-negative construct of IRAK-1. (C) Restored LPS responsiveness of tolerant epithelial cells by overexpression of IRAK-1. Naive and tolerant m-IC_{cl2} cells were left untreated or transfected with a control or IRAK-1 expression construct before second stimulation. Significant reduction ($P < 0.01$) of MIP-2 secretion in tolerant cells was observed in mock or pFlag-transfected but not in pIRAK-1–transfected cells. (D) Immunoblot demonstrating IRAK-1 levels in naive cells as well as in tolerant mock-, pFlag-, and pIRAK-1–transfected cells. (E) Immunostaining for the NF-κB subunit p65 (red) showing nuclear translocation in naive cells as well as pIRAK-1–transfected (green) tolerant cells in response to LPS stimulation. n.s., not significant. Counterstaining with DAPI. Bar, 40 μm.

who are unable to mount an adequate negative regulatory control. The further elucidation of the described tolerance acquisition process and characterization of all regulatory mechanisms involved will certainly help to reveal a more detailed picture of innate immune recognition within the gastrointestinal tract and its possible role in the pathogenesis of inflammatory diseases.

MATERIALS AND METHODS

Antibodies and reagents. Rat monoclonal anti-TLR4/MD-2 antibodies (MTS510) and mouse monoclonal antibodies to *Salmonella* O4 and O5 antigen were generously provided by K. Miyake (Saga Medical School, Nabeshima, Saga, Japan) and M. Kim (Kim Laboratories Inc.), respectively. Rabbit anti–MIP-2 antiserum was purchased from Nordic Biosite. The mouse monoclonal anti-phospho–IκB-α (Ser32/36) antibody and the rabbit polyclonal anti-phospho–NF-κB p65 (Ser536) antibody were from Cell Signaling Technology, and the rabbit polyclonal anti-actin antiserum was from Sigma-Aldrich. The mouse monoclonal anti–IRAK-1 antibody was obtained from Santa Cruz Biotechnology, Inc., and the rabbit polyclonal anti–IRAK-1 antibody plus the corresponding blocking peptide was from LabVision Corporation. The NF-κB reporter construct pBIIX-luciferase carrying two copies (2× NF-κB) of the κB sequences from the Igκ enhancer was provided by S. Ghosh (Yale University Medical School, New Haven, CT). The dominant-negative and wild-type IRAK-1 expression construct was provided by M. Muzio (Instituto di Ricerche Farmacologiche Mario Negri, Milano, Italy) and Amgen, respectively. The ubiquitin expression plasmid was provided by K. Lindsten (Karolinska Institute, Stockholm, Sweden). Murine recombinant IL-1β was purchased from Nordic Biosite, and TNF was from R&D Systems. *Escherichia coli* K12 D31m4 LPS was ordered from List Biological Laboratories. Purity of the LPS preparation was confirmed by complete absence of stimulating activity on peritoneal macrophages isolated from TLR4-deficient mice and preserved potency after repeated phenol-chloroform extractions (not depicted). LPS was quantified using the chromogenic QCL-1000 limulus amebocyte lysate system from BioWhittaker. *S. typhimurium* LPS and brefeldin A were purchased from Sigma-Aldrich. The kinase inhibitor K-252b was purchased from Alexis Biochemicals. The chemokines MIP-2, TNF, and KC were quantified using commercial ELISAs from Nordic Biosite and R&D Systems, respectively. Rat tail collagen was ordered from Institute Jacques Boy. Cell culture reagents were all from Gibco Life Technologies if not stated otherwise.

Mice and primary cell isolation. C57BL/6 mice were purchased from Charles River Breeding Laboratories, housed under specific pathogen-free conditions, and treated in accordance with the local animal protection legislation (Regierungspräsidium Stuttgart). The TLR4-deficient C57BL/10ScN mice were provided by M. Freudenberg (Max Planck-Institute of Immunobiology, Freiburg, Germany). Mice were killed and the small intestine was removed and extensively rinsed with ice-cold PBS. The intestinal epithelium was separated from the underlying tissue by incubation in 30 mM EDTA in Ca^{2+}- and Mg^{2+}-free PBS for 10 min at 37°C followed by vigorous shaking. Cells were harvested by centrifugation, washed, and multicellular epithelial aggregates were purified by repeated differential sedimentation at 1*g* in ice-cold PBS from contaminating cells and residual tissue. Viability of adult primary IECs was illustrated by rapid phosphorylation of STAT6 upon incubation in the presence of 10 ng/ml IL-4 or IL-13 (not depicted). Small intestinal tissue of neonatal mice was obtained from spontaneously delivered newborns. Caesarean section was performed with full-term gravid females, and newborn mice were killed immediately or kept separately under infrared light for 2 h after delivery. Intestinal macrophages were separated from EDTA-treated intestinal tissue using a 100-μm nylon cell strainer (BD Falcon) and enriched by adhesion to plastic cell culture plates for 2 h at 37°C. Blood monocytes were obtained from newborn mice, and cytokine secretion was determined in a whole blood assay. Peritoneal macrophages were harvested after intraperitoneal injection of sterile 4% Brewer's thioglycolate broth (Sigma-Aldrich).

Cell culture and stimulation assays. Primary IECs were cultured in a modified, hormonally defined medium with DMEM and F12 (vol 1:1) supplemented with 5% FCS (PAA), 2% glucose, 20 mM Hepes, 2 mM glutamin, 5 μg/ml insulin, 50 nM dexamethasone, 60 nM sodium selenite, 10 ng/ml epithelial growth factor, 5 μg/ml transferrin, and 1 nM 3,3′,5-triiodo-L-thyronine sodium salt as described previously (38). To prevent microbial growth, 100 U/ml penicillin, 100 μg/ml streptomycin, and 2.5 μg/ml amphotericin B (Sigma-Aldrich) were added. Cells were incubated at 37°C in a 5% CO_2/95% humidity air atmosphere on collagen-coated cell culture dishes. Primary intestinal macrophages or blood monocytes were cultured in RPMI 1640 medium supplemented with 5% FCS (PAA), 100 U/ml penicillin, and 100 μg/ml streptomycin (Invitrogen). Murine small intestinal epithelial m-IC_{cl2} cells were cultured as described previously (6, 39). RAW 264.7 cells were obtained from the American Type Culture Collection and propagated in RPMI 1640 medium (Invitrogen) supplemented with 20 mM Hepes, 2 mM L-glutamine, and 10% FCS. Plasmid DNA was prepared using the EndoFree Plasmid kit from QIAGEN, and transfection was performed using Lipofectamine 2000 reagent (Invitrogen) according to the manufacturer's instructions. Stimulation was performed by the addition of 50 ng/ml TNF, 100 ng/ml IL-1β, or LPS at the indicated concentrations. Cell culture supernatants were harvested after 12 h and stored at −20°C until further analysis. For kinase inhibition, m-IC_{cl2} cells were preincubated for 40 min in the presence of 25 μM K-252b and subsequently stimulated with 100 ng/ml LPS for 2 h. 5 μg of total cell lysate was analyzed by Western blot for the presence of IRAK-1.

Immunofluorescence staining of cells and tissue sections. Staining of primary IECs for ZO-1 and E-cadherin was performed using a rabbit anti–ZO-1 antiserum (Zymed Laboratories) and the mouse monoclonal IgG_{2a} anti–E-cadherin antibody (BD Transduction Laboratories), respectively, followed by the appropriate Cy3-conjugated secondary antibodies (Jackson ImmunoResearch Laboratories). Actin staining in primary IECs was performed by incubation with FITC-phalloidin 1:200 (Sigma-Aldrich) for 10 min. Immunolabeling of internalized *S. typhimurium* LPS was performed after fixation in 3.5% paraformaldehyde and permeabilization with 0.5% saponin using two mouse monoclonal anti-O4 and anti-O5 antibodies simultaneously, followed by incubation with a Cy3-conjugated goat anti–mouse secondary antibody (Jackson ImmunoResearch Laboratories). Intracellular staining for MIP-2 in primary IECs was performed after permeabilization with 0.5% saponin after a 6-h incubation with 0.5 μg/ml brefeldin A. Bound MIP-2 antibodies were detected using a goat anti–rabbit Cy3-conjugated antibody (Jackson ImmunoResearch Laboratories). Cellular distribution of the NF-κB subunit p65 in situ was analyzed by immunofluorescence using a rabbit anti–NF-κB p65 antiserum (Santa Cruz Biotechnology, Inc.). Cryosections were acetone-fixed, blocked with 10% normal donkey serum, and incubated with primary antibody at a 1:50 dilution for 1 h. After washing, antibody binding was visualized using a Texas Red–conjugated donkey anti–rabbit antiserum (Jackson ImmunoResearch Laboratories). Immunostaining for $CD45^+$ cells was performed using biotin-conjugated rat anti-CD45 antibodies in combination with FITC-labeled streptavidin (BD Biosciences). Vectashield-mounted slides (Vector Laboratories) were visualized using an ApoTome-equipped Axioplan 2 microscope connected to an AxioCam M_r digital camera (Carl Zeiss MicroImaging, Inc.). Immunostaining of phosphorylated IκB-α in paraformaldehyde-fixed intestinal tissue sections was performed using a phospho–IκB-α Ser32/36-specific mouse monoclonal antibody (Cell Signaling Technology) exactly as described in the manufacturers' recommendations. The Vectastain Elite ABC-kit (Vector Laboratories) in combination with a biotinylated goat anti–mouse $(Fab')_2$ antiserum (Jackson ImmunoResearch Laboratories) and the DAB substrate kit with 3′,3′-diaminobenzidine (Vector Laboratories) was used for visualization.

Immunoblotting and immunoprecipitation. Cell lines and isolated primary IECs were resuspended in lysis buffer (3:1 WB/SB vol/vol; SB: 250 mM Tris, pH 6.5, 8% SDS, 40% glycerol; WB: 50 mM Tris, pH 7.4, 120 mM NaCl) supplemented with a proteinase inhibitor cocktail (Complete

Mini; Roche Diagnostics). Intestinal tissue was grinded to powder in liquid nitrogen and subsequently resuspended in 200 μl lysis buffer. Samples were sonified and the protein concentration was determined (DC Protein Assay; Bio-Rad Laboratories). For immunoprecipitation, cells were transfected with an ubiquitin expression plasmid 24 h before LPS stimulation (100 ng/ml, 0.5 h). Unstimulated and stimulated cells were lysed in buffer I (50 mM Tris-HCl, pH 7.5, 150 mM NaCl, 0.5% Nonidet P-40, 0.25% sodium-deoxycholate, proteinase inhibitor cocktail), sonified, centrifuged, and precleared with 50 μl protein G sepharose (GE Healthcare) for 3 h at 4°C. 1 μg mouse monoclonal anti-ubiquitin antiserum (Sigma-Aldrich) was added to the precleared supernatant for 1 h at 4°C, followed by the addition of 50 μl protein G sepharose and incubation overnight at 4°C. Bound protein was washed twice in lysis buffer (I), followed by two washing steps in buffer II (similar to buffer I, but 250 mM NaCl, 0.1% Nonidet P-40, 0.025% sodium-deoxycholate) and one washing step in buffer III (similar to buffer I, but 0.1% Nonidet P-40, 0.025% sodium-deoxycholate). Protein was eluted in loading buffer and separated on a 10% acrylamide gel and blotted on nitrocellulose. Membranes were incubated overnight at 4°C with the primary antibody at the recommended concentration. Detection was performed using peroxidase-labeled goat anti–mouse or goat anti–rabbit secondary antibodies (Jackson ImmunoResearch Laboratories) in combination with the ECL kit (GE Healthcare). Before restaining, membranes were stripped for 45 min at 50°C in 62.5 mM Tris HCl, pH 6.7, 100 mM β-mercaptoethanol, and 2% SDS, followed by three 15-min washing steps.

Flow cytometry. Before flow cytometry, ex vivo–isolated primary IEC aggregates were trypsinized to obtain single cell suspensions. Analysis for contaminating hematopoietic cells was performed using FITC-conjugated anti-CD3 and anti-CD11b, PE-conjugated anti-B220, and biotin-conjugated anti-CD45 antibodies as well as APC-conjugated streptavidin (all purchased from BD Biosciences). Apoptosis was determined using FITC-annexin (BD Biosciences) according to the manufacturer's protocol. TLR4/MD-2 expression was visualized using a goat anti–rat FITC-conjugated secondary antibody (Jackson ImmunoResearch Laboratories) after fixation (Cytofix; BD Biosciences) with or without permeabilization in Ca^{2+}- and Mg^{2+}-free PBS containing 0.5% saponin and 2% FCS. Rat anti-haemagglutinin monoclonal antibodies (Boehringer) were used as isotype control. MIP-2 production was determined by intracellular cytokine staining after a 6-h incubation with 0.5 μg/ml brefeldin A (Sigma-Aldrich) in the presence or absence of 100 ng/ml LPS. Primary IECs were then trypsinized, fixed (Cytofix; BD Biosciences), and permeabilized. Cells were incubated on ice with rabbit anti–MIP-2 antiserum (1:100; Nordic Biosite) in PBS, 1% FCS and 0.5% saponin, and then washed and stained using a goat Cy5-conjugated anti–rabbit IgG (Jackson ImmunoResearch Laboratories). An isotype monoclonal mouse IgG2a antibody was used as isotype control for the anti–E-cadherin antibody (BD Biosciences). Intestinal macrophages were characterized using PE-conjugated anti-CD45, anti-BM8, and anti-CD40 as well as biotin-conjugated anti-B7.1 antibodies in combination with streptavidin-PE (BD Biosciences). Cells were analyzed on a FACSCalibur apparatus (BD Biosciences).

Laser microdissection and RT-PCR analysis. Total epithelial RNA was isolated from intestinal tissue by laser microdissection (AS LMD; Leica) using a standard protocol. In brief, 10-μm sections from snap-frozen intestinal tissue were placed on RNase ZAP (Sigma-Aldrich) -pretreated PET frame slides, air-dried, fixed, and stained with 0.1% toluidine blue in DEPC water. Epithelial cells were collected and subjected to RNA isolation (RNeasy Micro kit; QIAGEN). Total RNA from small intestinal tissue or primary IEC preparations was isolated using TRIzol reagent (Invitrogen) according to the manufacturer's protocol. cDNA was synthesized from total mRNA using oligo$(dT)_{18}$ primer from the first-strand cDNA synthesis AMV kit (Roche). The following primers were used for DNA amplification: *β_2 microglobulin* (forward: 5′-GCTCGGTGACCCTGGTCTTT-3′, reverse: 5′-AATGTGAGGCGGGTGGAACT-3′); *Hprt* (forward: 5′-TGATCAGTCAACGGGGGACA-3′, reverse: 5′-TTCGAGAGGTCCTTTTCACCA-3′); *Tlr4* (forward: 5′-TGGCTCCTGGCTAGGACTCTG-3′, reverse: 5′-TCTTCAAGGGGTTGAAGCTCAG-3′); *Md-2* (forward: 5′-TGCAACTCCTCCGATGCAAT-3′, reverse: 5′-TTCCTTACGCTTCGGCAACTC-3′); *Tollip* (forward: 5′-GCAGGGTGTTGGCTATGTGC-3′, reverse: 5′-TCCCTGTCCATGTTGGGAAA-3′); *Sigirr* (forward: 5′-GCTGACCTCCTGATGGCTGA-3′, reverse: 5′-GCAGGGCGAGCAAGAAGTC-3′); *ST-2* (forward: 5′-TCCCATGTATTTGACAGTTACGG-3′, reverse: 5′-CAGCTTGGCGGCTTTTTATG-3′); *Irak-1* (forward: 5′-GAGGATCAGCTCCACCTTCA-3′, reverse: 5′-GGGTACCTCGAACTGTGGAA-3′); *Cd45* (forward: 5′-GCTCAAACTTCTGGCCTTTG-3′, reverse: 5′-AGCACATGTTTGCTTCGTTG-3′); and *Myd88/sMyD88* (forward: 5′-AGAGCTGCTGGCCTTGTTAG-3′, reverse: 5′-TCATCTCCTGCACAAACTCG-3′). The MyD88 primers used were designed to span the domain that is missing in the short form of MyD88 (sMyD88) and therefore resulted in a 266- or 130-nucleotide-long amplificate for the complete or alternatively spliced short form of MyD88, respectively, as published previously (18). All primers used in this study were intron spanning as demonstrated by the absence of amplification from genomic DNA. Sequencing of all PCR products confirmed the specificity of the primers used. For quantitative mRNA analysis, the reaction mixture was prepared using 2× Taqman Universal Mastermix (Applied Biosystems), sample cDNA, intron-spanning forward and reverse primers, as well as the 6-carboxy-fluorescein–conjugated target probe provided in the commercial TaqMan gene expression assay for murine hypoxanthine phosphoribosyltransferase (HPRT) and MIP-2 (Applied Biosystems). PCR amplification and detection were performed using an ABI Prism 7900 sequence detector (Applied Biosystems) according to the manufacturer's instructions. Each sample was amplified in triplicate and normalized to the endogenous HPRT control. Values are indicated as relative quantities (RQs) to the calibrator sample represented by the fetal or postnatal intestinal tissue sample ± the minimal and maximal RQ value of the measurement.

Statistical analysis. Results are given as the mean ± SD. Statistical analyses were performed using the Student's *t* test. A p-value <0.05 was considered significant.

We are indebted to those who provided expression constructs and reagents. We thank Dr. Kirsch (Department of Anatomy, University of Freiburg, Germany) for the access to the laser microdissection microscope and technical advice. The TLR4-deficient mice were generously provided by Professor Marina Freudenberg (Freiburg, Germany).

This work was supported by grants from the German Research Foundation (DFG grant HO 2236/5-1 to M.W. Hornef), the Swedish Research Council (K2003-31P-14792 to M.W. Hornef), Cancerfonden (to M.W. Hornef), the University of Freiburg (to M.W. Hornef), and the Fondation de la Recherche Médical (FRM to S. Ménard).

The authors have no conflicting financial interests.

Submitted: 25 March 2005
Accepted: 10 March 2006

REFERENCES

1. Hooper, L.V., J. Xu, P.G. Falk, T. Midtvedt, and J.I. Gordon. 1999. A molecular sensor that allows a gut commensal to control its nutrient foundation in a competitive ecosystem. *Proc. Natl. Acad. Sci. USA*. 96:9833–9838.
2. Medzhitov, R. 2001. Toll-like receptors and innate immunity. *Nat. Rev. Immunol.* 1:135–145.
3. Abreu, M.T., P. Vora, E. Faure, L.S. Thomas, E.T. Arnold, and M. Arditi. 2001. Decreased expression of Toll-like receptor-4 and MD-2 correlates with intestinal epithelial cell protection against dysregulated proinflammatory gene expression in response to bacterial lipopolysaccharide. *J. Immunol.* 167:1609–1616.
4. Naik, S., E.J. Kelly, L. Meijer, S. Pettersson, and I.R. Sanderson. 2001. Absence of Toll-like receptor 4 explains endotoxin hyporesponsiveness in human intestinal epithelium. *J. Pediatr. Gastroenterol. Nutr.* 32:449–453.

5. Cario, E., I.M. Rosenberg, S.L. Brandwein, P.L. Beck, H.C. Reinecker, and D.K. Podolsky. 2000. Lipopolysaccharide activates distinct signaling pathways in intestinal epithelial cell lines expressing Toll-like receptors. *J. Immunol.* 164:966–972.
6. Hornef, M.W., T. Frisan, A. Vandewalle, S. Normark, and A. Richter-Dahlfors. 2002. Toll-like receptor 4 resides in the Golgi apparatus and colocalizes with internalized lipopolysaccharide in intestinal epithelial cells. *J. Exp. Med.* 195:559–570.
7. Zhang, D., G. Zhang, M.S. Hayden, M.B. Greenblatt, C. Bussey, R.A. Flavell, and S. Ghosh. 2004. A Toll-like receptor that prevents infection by uropathogenic bacteria. *Science.* 303:1522–1526.
8. Armstrong, L., A.R. Medford, K.M. Uppington, J. Robertson, I.R. Witherden, T.D. Tetley, and A.B. Millar. 2004. Expression of functional Toll-like receptor-2 and -4 on alveolar epithelial cells. *Am. J. Respir. Cell Mol. Biol.* 31:241–245.
9. Rakoff-Nahoum, S., J. Paglino, F. Eslami-Varzaneh, S. Edberg, and R. Medzhitov. 2004. Recognition of commensal microflora by Toll-like receptors is required for intestinal homeostasis. *Cell.* 118:229–241.
10. Fukata, M., K.S. Michelsen, R. Eri, L.S. Thomas, B. Hu, K. Lukasek, C.C. Nast, J. Lechago, R. Xu, Y. Naiki, et al. 2005. Toll-like receptor-4 is required for intestinal response to epithelial injury and limiting bacterial translocation in a murine model of acute colitis. *Am. J. Physiol. Gastrointest. Liver Physiol.* 288:G1055–G1065.
11. Pull, S.L., J.M. Doherty, J.C. Mills, J.I. Gordon, and T.S. Stappenbeck. 2005. Activated macrophages are an adaptive element of the colonic epithelial progenitor niche necessary for regenerative responses to injury. *Proc. Natl. Acad. Sci. USA.* 102:99–104.
12. Bjerknes, M., and H. Cheng. 1981. Methods for the isolation of intact epithelium from the mouse intestine. *Anat. Rec.* 199:565–574.
13. Cano-Gauci, D.F., J.C. Lualdi, A.J. Ouellette, G. Brady, N.N. Iscove, and R.N. Buick. 1993. In vitro cDNA amplification from individual intestinal crypts: a novel approach to the study of differential gene expression along the crypt-villus axis. *Exp. Cell Res.* 208:344–349.
14. Hornef, M.W., B.H. Normark, A. Vandewalle, and S. Normark. 2003. Intracellular recognition of lipopolysaccharide by Toll-like receptor 4 in intestinal epithelial cells. *J. Exp. Med.* 198:1225–1235.
15. Smythies, L.E., M. Sellers, R.H. Clements, M. Mosteller-Barnum, G. Meng, W.H. Benjamin, J.M. Orenstein, and P.D. Smith. 2005. Human intestinal macrophages display profound inflammatory anergy despite avid phagocytic and bacteriocidal activity. *J. Clin. Invest.* 115:66–75.
16. Wald, D., J. Qin, Z. Zhao, Y. Qian, M. Naramura, L. Tian, J. Towne, J.E. Sims, G.R. Stark, and X. Li. 2003. SIGIRR, a negative regulator of Toll-like receptor-interleukin 1 receptor signaling. *Nat. Immunol.* 4:920–927.
17. Brint, E.K., D. Xu, H. Liu, A. Dunne, A.N. McKenzie, L.A. O'Neill, and F.Y. Liew. 2004. ST2 is an inhibitor of interleukin 1 receptor and Toll-like receptor 4 signaling and maintains endotoxin tolerance. *Nat. Immunol.* 5:373–379.
18. Burns, K., S. Janssens, B. Brissoni, N. Olivos, R. Beyaert, and J. Tschopp. 2003. Inhibition of interleukin 1 receptor/Toll-like receptor signaling through the alternatively spliced, short form of MyD88 is due to its failure to recruit IRAK-4. *J. Exp. Med.* 197:263–268.
19. Otte, J.M., E. Cario, and D.K. Podolsky. 2004. Mechanisms of cross hyporesponsiveness to Toll-like receptor bacterial ligands in intestinal epithelial cells. *Gastroenterology.* 126:1054–1070.
20. Jacinto, R., T. Hartung, C. McCall, and L. Li. 2002. Lipopolysaccharide- and lipoteichoic acid-induced tolerance and cross-tolerance: distinct alterations in IL-1 receptor-associated kinase. *J. Immunol.* 168:6136–6141.
21. Sato, S., O. Takeuchi, T. Fujita, H. Tomizawa, K. Takeda, and S. Akira. 2002. A variety of microbial components induce tolerance to lipopolysaccharide by differentially affecting MyD88-dependent and -independent pathways. *Int. Immunol.* 14:783–791.
22. Medvedev, A.E., A. Lentschat, L.M. Wahl, D.T. Golenbock, and S.N. Vogel. 2002. Dysregulation of LPS-induced Toll-like receptor 4-MyD88 complex formation and IL-1 receptor-associated kinase 1 activation in endotoxin-tolerant cells. *J. Immunol.* 169:5209–5216.
23. Yamin, T.T., and D.K. Miller. 1997. The interleukin-1 receptor-associated kinase is degraded by proteasomes following its phosphorylation. *J. Biol. Chem.* 272:21540–21547.
24. Kanakaraj, P., P.H. Schafer, D.E. Cavender, Y. Wu, K. Ngo, P.F. Grealish, S.A. Wadsworth, P.A. Peterson, J.J. Siekierka, C.A. Harris, and W.P. Fung-Leung. 1998. Interleukin (IL)-1 receptor–associated kinase (IRAK) requirement for optimal induction of multiple IL-1 signaling pathways and IL-6 production. *J. Exp. Med.* 187:2073–2079.
25. Kanakaraj, P., K. Ngo, Y. Wu, A. Angulo, P. Ghazal, C.A. Harris, J.J. Siekierka, P.A. Peterson, and W.P. Fung-Leung. 1999. Defective interleukin (IL)-18–mediated natural killer and T helper cell type 1 responses in IL-1 receptor–associated kinase (IRAK)-deficient mice. *J. Exp. Med.* 189:1129–1138.
26. Thomas, J.A., J.L. Allen, M. Tsen, T. Dubnicoff, J. Danao, X.C. Liao, Z. Cao, and S.A. Wasserman. 1999. Impaired cytokine signaling in mice lacking the IL-1 receptor-associated kinase. *J. Immunol.* 163:978–984.
27. Medzhitov, R., P. Preston-Hurlburt, and C.A. Janeway Jr. 1997. A human homologue of the Drosophila Toll protein signals activation of adaptive immunity. *Nature.* 388:394–397.
28. Edwards, C.A., and A.M. Parrett. 2002. Intestinal flora during the first months of life: new perspectives. *Br. J. Nutr.* 88:S11–S18.
29. Backhed, F., and M. Hornef. 2003. Toll-like receptor 4-mediated signaling by epithelial surfaces: necessity or threat? *Microbes Infect.* 5:951–959.
30. Schilling, J.D., S.M. Martin, C.S. Hung, R.G. Lorenz, and S.J. Hultgren. 2003. Toll-like receptor 4 on stromal and hematopoietic cells mediates innate resistance to uropathogenic *Escherichia coli*. *Proc. Natl. Acad. Sci. USA.* 100:4203–4208.
31. Andonegui, G., C.S. Bonder, F. Green, S.C. Mullaly, L. Zbytnuik, E. Raharjo, and P. Kubes. 2003. Endothelium-derived Toll-like receptor-4 is the key molecule in LPS-induced neutrophil sequestration into lungs. *J. Clin. Invest.* 111:1011–1020.
32. Janssens, S., and R. Beyaert. 2003. Functional diversity and regulation of different interleukin-1 receptor-associated kinase (IRAK) family members. *Mol. Cell.* 11:293–302.
33. Li, X., M. Commane, C. Burns, K. Vithalani, Z. Cao, and G.A. Stark. 1999. Mutant cells that do not respond to interleukin-1 (IL-1) reveal a novel role for IL-1 receptor-associated kinase. *Mol. Cell. Biol.* 19:4643–4652.
34. Chan, K.L., J.C. Ho, K.W. Chan, and P.K. Tam. 2002. A study of gut immunity to enteral endotoxin in rats of different ages: a possible cause for necrotizing enterocolitis. *J. Pediatr. Surg.* 37:1435–1440.
35. Nanthakumar, N.N., R.D. Fusunyan, I. Sanderson, and W.A. Walker. 2000. Inflammation in the developing human intestine: a possible pathophysiologic contribution to necrotizing enterocolitis. *Proc. Natl. Acad. Sci. USA.* 97:6043–6048.
36. Fusunyan, R.D., N.N. Nanthakumar, M.E. Baldeon, and W.A. Walker. 2001. Evidence for an innate immune response in the immature human intestine: Toll-like receptors on fetal enterocytes. *Pediatr. Res.* 49:589–593.
37. Hsueh, W., M.S. Caplan, X.W. Qu, X.D. Tan, I.G. De Plaen, and F. Gonzalez-Crussi. 2003. Neonatal necrotizing enterocolitis: clinical considerations and pathogenetic concepts. *Pediatr. Dev. Pathol.* 6:6–23.
38. Claud, E.C., L. Lu, P.M. Anton, T. Savidge, W.A. Walker, and B.J. Cherayil. 2004. Developmentally regulated Iκ-B expression in intestinal epithelium and susceptibility to flagellin-induced inflammation. *Proc. Natl. Acad. Sci. USA.* 101:7404–7408.
39. Bens, M., A. Bogdanova, F. Cluzeaud, L. Miquerol, S. Kerneis, J.P. Kraehenbuhl, A. Kahn, E. Pringault, and A. Vandewalle. 1996. Transimmortalized mouse intestinal cells (m-IC_{c12}) that maintain a crypt phenotype. *Am. J. Physiol.* 270:C1666–C1674.